Journal of
Applied Physics

Optical absorption and oxygen passivation of surface states in III-nitride photonic devices

Cite as: J. Appl. Phys. **123**, 113103 (2018); https://doi.org/10.1063/1.5022150
Submitted: 11 January 2018 . Accepted: 03 March 2018 . Published Online: 19 March 2018

Ian Rousseau, Gordon Callsen, Gwénolé Jacopin, Jean-François Carlin, Raphaël Butté, and Nicolas Grandjean

COLLECTIONS

EP This paper was selected as an Editor's Pick

ARTICLES YOU MAY BE INTERESTED IN

Burying non-radiative defects in InGaN underlayer to increase InGaN/GaN quantum well efficiency
Applied Physics Letters **111**, 262101 (2017); https://doi.org/10.1063/1.5007616

Optical absorption edge broadening in thick InGaN layers: Random alloy atomic disorder and growth mode induced fluctuations
Applied Physics Letters **112**, 032106 (2018); https://doi.org/10.1063/1.5010879

GaN surface as the source of non-radiative defects in InGaN/GaN quantum wells
Applied Physics Letters **113**, 111106 (2018); https://doi.org/10.1063/1.5048010

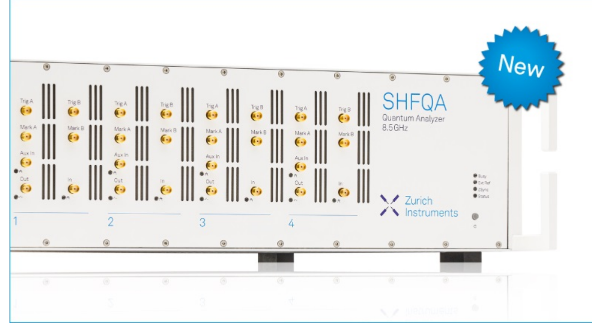

Your Qubits. Measured.
Meet the next generation of quantum analyzers
- Readout for up to 64 qubits
- Operation at up to 8.5 GHz, mixer-calibration-free
- Signal optimization with minimal latency
Find out more

© 2018 Author(s).

JOURNAL OF APPLIED PHYSICS 123, 113103 (2018)

Optical absorption and oxygen passivation of surface states in III-nitride photonic devices

Ian Rousseau,[a] Gordon Callsen, Gwénolé Jacopin, Jean-François Carlin, Raphaël Butté, and Nicolas Grandjean

Institute of Physics, École Polytechnique Fédérale de Lausanne (EPFL), CH-1015 Lausanne, Switzerland

(Received 11 January 2018; accepted 3 March 2018; published online 19 March 2018)

III-nitride surface states are expected to impact high surface-to-volume ratio devices, such as nano- and micro-wire light-emitting diodes, transistors, and photonic integrated circuits. In this work, reversible photoinduced oxygen desorption from III-nitride microdisk resonator surfaces is shown to increase optical attenuation of whispering gallery modes by $100\,\text{cm}^{-1}$ at $\lambda = 450\,\text{nm}$. Comparison of photoinduced oxygen desorption in unintentionally and n^+-doped microdisks suggests that the spectral changes originate from the unpinning of the surface Fermi level, likely taking place at etched nonpolar III-nitride sidewalls. An oxygen-rich surface prepared by thermal annealing results in a broadband Q improvement to state-of-the-art values exceeding 1×10^4 at 2.6 eV. Such findings emphasize the importance of optically active surface states and their passivation for future nanoscale III-nitride optoelectronic and photonic devices. © *2018 Author(s). All article content, except where otherwise noted, is licensed under a Creative Commons Attribution (CC BY) license (http://creativecommons.org/licenses/by/4.0/).* https://doi.org/10.1063/1.5022150

I. INTRODUCTION

The proliferation of III-nitride semiconductor optoelectronics for solid-state lighting has encouraged research and development of small length scale devices for new applications. Examples include nanowire light-emitting diodes (LEDs) for lighting[1] and nanolasers,[2] high frequency transistors for power electronics,[3,4] and nanophotonics for photonic integrated circuits.[5] However, these additional application opportunities for small devices are paid at the expense of an increased surface-to-volume ratio. In the case of optoelectronic and photonic devices, surface absorption is expected to gain relative importance as one or more physical dimensions approach the wavelength of light in the material.

Surface states usually result from the termination of an infinite periodic semiconductor lattice. Such states, characterized by spatial localization at the surface, may have energies falling within the electronic band gap of the bulk crystal and exhibit crystal orientation dependence due to the directionality of covalent bonds.[6] Since any practical device must be connected to the outside world by at least one interface, surface states and their passivation have been investigated extensively for applications ranging from Schottky contact optimization[7] to the minimization of surface recombination in optoelectronics.[8] Compared to the half century of development in silicon and III-arsenide semiconductors, passivation techniques for the decades-old III-nitride semiconductors remain an ongoing research topic.

Material-specific surface treatments greatly benefited nano-optical resonators fabricated from silicon[9] and gallium arsenide.[10] In such resonators, an optical cavity with wavelength scale dimensions is constructed by patterning the high refractive index semiconductor into disk[11] or photonic crystal geometries.[12,13] The electromagnetic standing waves in the resonator exhibit high electric field intensity at the semiconductor-air interface, enhancing the interaction between the optical wave and the surface.[14] Generally, the quality factor $Q = E_0/\Delta E$ serves as the resonator figure-of-merit, where E_0 is the resonance energy and ΔE is its full width at half maximum (FWHM). Various broadening mechanisms diminish the experimental Q, which, for nanophotonic resonators at short wavelengths, substantially departs from that calculated by theory.[15,16] The loss contributions are typically accounted for by the empirical formula $Q^{-1} = Q_{th}^{-1} + Q_{abs}^{-1} + Q_{sc}^{-1}$, where Q_{th} is the Q factor derived from theoretical electromagnetic calculations, Q_{abs} describes the contribution from both bulk and surface state absorption, and Q_{sc} accounts for scattering loss caused by surface roughness.[17]

Past research on GaN-based nanophotonic structures has identified several candidate loss channels that may limit experimental Q at high energies or short wavelengths (2.5–3 eV/400–500 nm). Such issues may also apply to recent AlN-based photonic devices designed for the UV.[18–20] In GaN, Puchtler *et al.* advocated a correlation between the dislocation defect density and experimental Q.[21] Other authors proposed residual absorption in bulk GaN[22] and/or surface roughness at short wavelengths as the main responsible mechanism.[23,24] We recently quantified losses in GaN photonic nanostructures and showed that the dominant loss mechanism is linked to the III-nitride semiconductor surface.[16] This work examines the impact of optically active surface states on whispering gallery resonances in III-nitride microdisks via reversible photoinduced oxygen desorption from the GaN surface.

II. EXPERIMENTAL SYSTEM

III-nitride microdisk resonators [Figs. 1(a) and 1(b)] are fabricated from III-nitride epilayers grown on silicon (111) in which a single InGaN/GaN quantum well (QW) serves as an internal light source. The microdisks are mounted in a

[a]ian.rousseau@epfl.ch

 © Author(s) 2018.

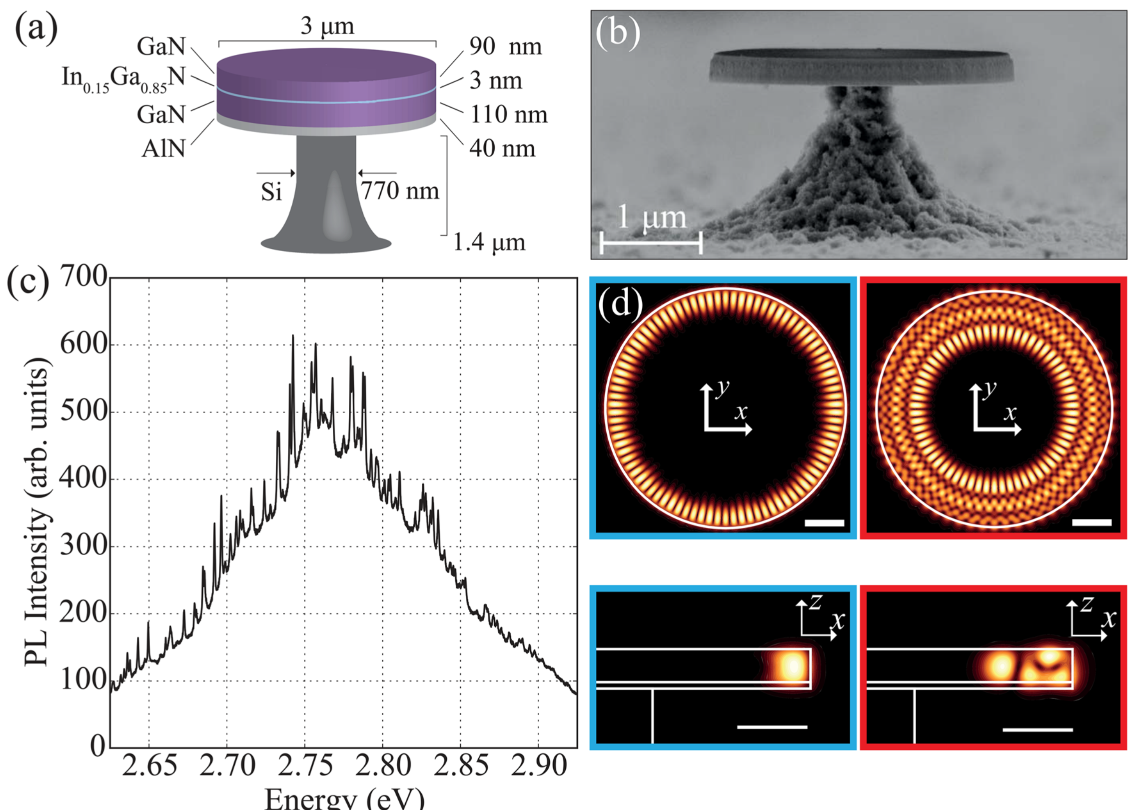

FIG. 1. Physical and optical properties of the studied microdisks. (a) Schematic of epilayer and microdisk dimensions employed in this study. (b) Scanning electron microscopy (SEM) image of the fabricated microdisk observed at 85° from the vertical. (c) Typical photoluminescence spectrum at 5 K under optical pumping at 460 W/cm^2 with a 325 nm cw laser. (d) Simulated electric field intensity profiles in the xy plane at the microdisk center (top) and xz (bottom) planes for modes calculated at 2.762 eV (blue) and 2.759 eV (red) shown for discussion purposes. The scale bars represent 500 nm.

commercial closed cycle helium cryostat (Cryostation C2 from Montana Instruments, Inc.) and are pumped nonresonantly by a continuous wave (cw) HeCd laser emitting at 325 nm using a UV microphotoluminescence (μPL) setup. Details about the sample growth, fabrication, and measurement apparatus can be found in the supplementary information.

Figure 1(c) shows a typical microdisk μPL spectrum measured at 5 K under 460 W/cm^2 illumination and high vacuum ($<1 \times 10^{-3}$ mbar). Microdisk resonances appear as sharp peaks superposed on a broad QW PL background. Modes on the high energy side of the QW peak diminish in relative intensity and broaden, likely due to absorption in the QW shifted by the quantum-confined Stark effect.[23,25] For a disk radius $R = 1.5\,\mu$m and effective refractive index $n_{eff} = 2.1$, the free spectral range is $\lambda^2/2\pi R n_{eff}$, approximately 64 meV (10 nm) at 2.8 eV/440 nm. Therefore, the high peak density can be attributed to two factors: the small silicon post diameter resulting in modes with multiple radial nodes and the large relative thickness of the epilayers ($\sim 3\lambda/n_{eff}$), resulting in modes with multiple vertical nodes. Based on the vertical position of the QW in the epilayer stack, the QW is expected to most strongly couple to the fundamental transverse electric (TE) polarized mode; however, coupling to higher odd-order TE modes and residual coupling to transverse magnetic (TM) modes cannot be excluded.[11]

μPL spectra of nominally identical microdisks do not exhibit the same peak number and positions. In order to investigate the causes of non-reproducibility, theoretical 3D finite-difference time-domain (3D-FDTD) simulations[26] incorporating the experimental epilayer thickness, disk geometry, and material refractive index reveal sensitivity to silicon post size fluctuations. This is likely caused by the high refractive index and loss in silicon in the blue ($\tilde{n} = 5.2 + 0.7i$ at 2.76 eV/450 nm).[27] Additionally, the combination of the tensile strain release in the as-grown epilayers at the free microdisk edges and possible asymmetry of the silicon post due to the fabrication process causes an upward bowing of the microdisk (<20 nm). Such complications preclude the identification of a specific experimental peak with a simulated electric field profile. Therefore, the simulated electric field intensity profiles in Fig. 1(d) serve as aids in the visualization of possible electromagnetic mode profiles and should not be associated with a specific experimental resonance. However, such simulations suggest that each mode should probe the surface and volume with different sensitivity as a result of varying normalized electric field intensities at the semiconductor surface.

III. RESULTS AND DISCUSSION

A. Photoinduced oxygen desorption

Under cw optical pumping at 4.6 kW/cm^2 under high vacuum ($<1 \times 10^{-3}$ mbar) at room temperature, the microdisk modes redshift and broaden over time as shown in Figs. 2(a, left panel) and 2(b) up to $t = 30$ min. The modes do not recover their original lineshape if left in vacuum in the dark, even after waiting for several hours. Furthermore, direct

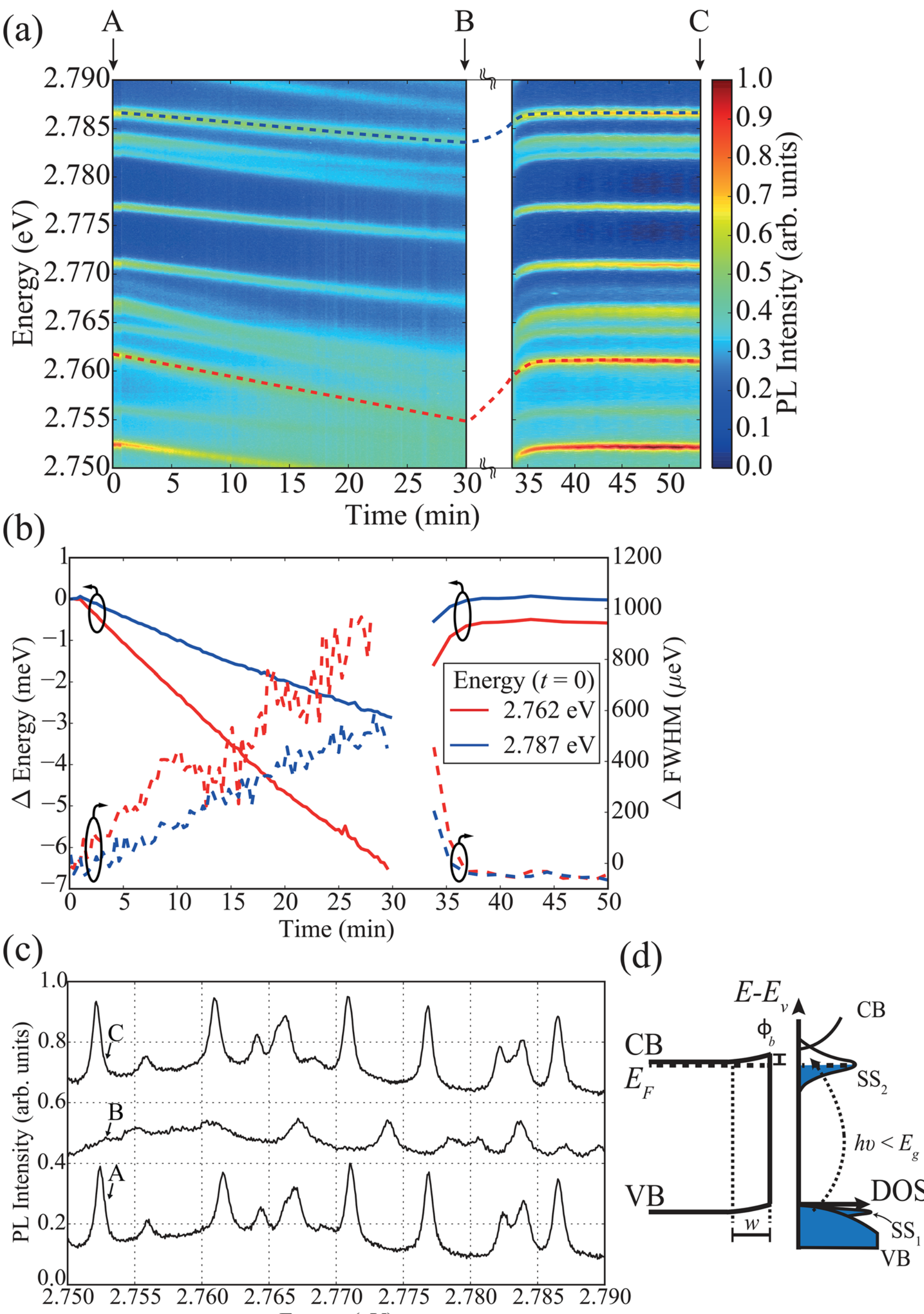

FIG. 2. Nearly reversible redshift and broadening of microdisk resonances caused by photoinduced desorption and adsorption of oxygen from III-nitride surfaces at room temperature. (a) Normalized PL time dependence under high vacuum ($<10^{-3}$ mbar) using optical pumping at 4.6 kW/cm^2 with a 325 nm cw laser shown with the quantum well PL background removed. At $t = 30$ min, O_2 is injected. (b) Linewidth and broadening extracted from Lorentzian lineshape fits for two selected modes. (c) μPL spectra at $t = 0$ (A), $t = 30$ (B), and $t = 54$ (C) minutes. (d) Schematic of upward band bending and density of states (DOS) due to Fermi level E_F pinning caused by a high density of unoccupied surface states (SS_2) below the conduction band (CB) minimum on the *m*-plane GaN surface in thermal equilibrium in the dark. A second filled band of surface states (SS_1) is expected below the valence band (VB) maximum.

temperature measurements by power-dependent Raman spectroscopy with the HeCd pump laser indicate that the apparent degradation cannot be ascribed to a thermal effect. Another striking feature is that the modes shift at different rates, likely due to the differing electric field intensity profiles [c.f. Fig. 1(d)].

Interestingly, the initial resonances are reestablished by the injection of 99.9999% pure oxygen gas into the cryostat at 100 mbar, as shown in Fig. 2(a, right panel). The evolution of the mode resonance spectrum after 0, 30′, and after recovery by oxygen injection (54′) is displayed in Fig. 2(c), showing the near complete reversibility of the photodesorption phenomenon in oxygen. As whispering gallery modes are sustained by the high refractive index contrast interface at the microdisk edge, the broadening and redshifting can be attributed to a change in the semiconductor's optical properties at the semiconductor-vacuum interface. Since the injection of oxygen restores the original optical spectrum, the spectral changes must be linked to oxygen adsorbed on the semiconductor surface. Any small differences in spectra at $t = 0$ and $t = 54'$ could be attributed to more complex surface physics which may alter the surface density of states, such as desorption of species other than oxygen or photoinduced chemisorption. Note that the UV-induced adsorption and desorption of oxygen gas has been observed previously on both $+c$- and m-plane GaN surfaces.[28,29]

Although the corresponding electric field intensity profiles remain unidentified, the broadening induced by oxygen desorption in Fig. 2(b) can be translated into a quantitative estimate of the change of absorption coefficient ($\Delta\alpha$). The

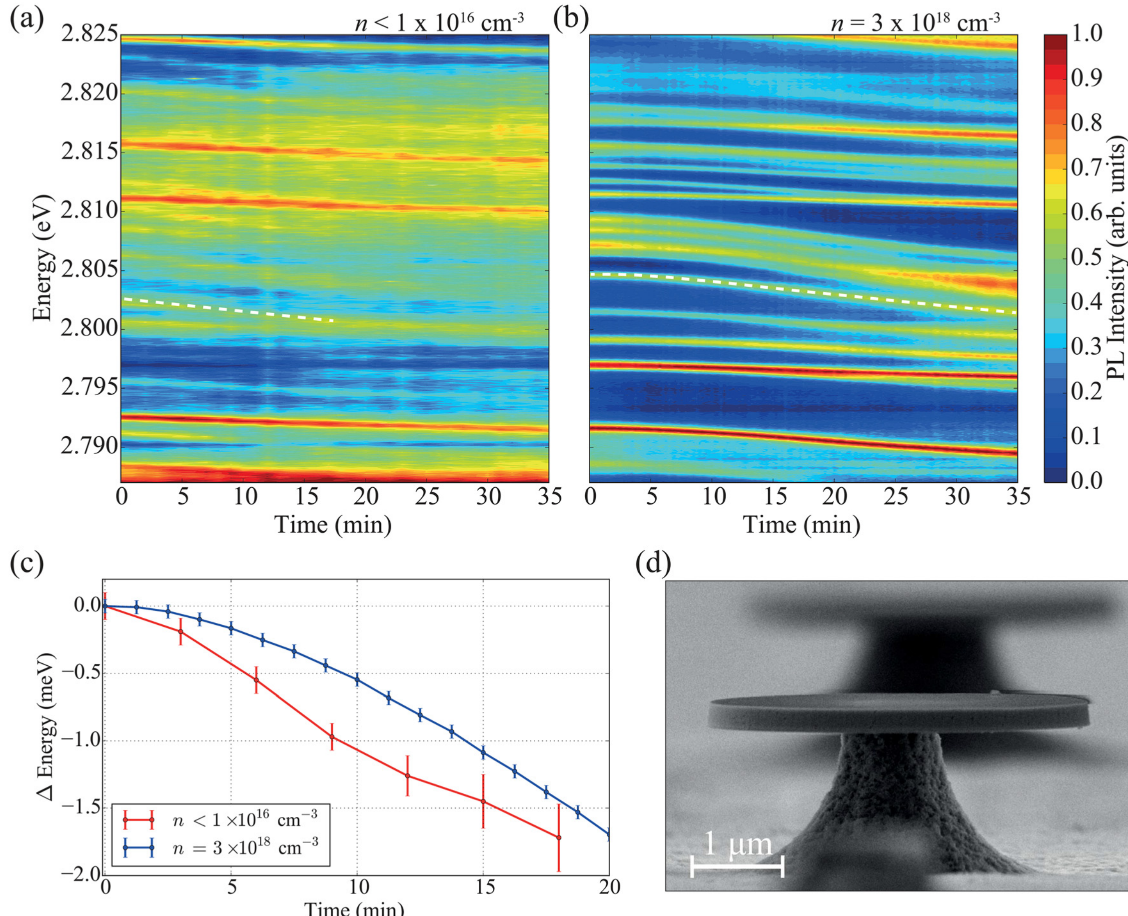

FIG. 3. Photoinduced desorption under high vacuum ($<1 \times 10^{-3}$ mbar) for 4.6 kW/cm^2 cw 325 nm illumination of microdisks fabricated from *nid* (a) and n^+ (b)-doped GaN epilayers. (c) Redshift time dependence for selected modes. (d) SEM profile of 4.0 μm diameter disks with 1.2 μm diameter silicon posts.

change in the quality factor $Q_{O_2}^{-1} = \Delta E_{O_2}/E_0$ is proportional to $\Delta\alpha$[30]

$$Q_{O_2}^{-1} = \frac{\lambda\,\Delta\alpha}{2\pi n_{eff}}. \qquad (1)$$

Evaluation of Eq. (1) using $E_0 = 2.762$ eV ($\lambda = 449.0$ nm), $n_{eff} = 2.1$, and $\Delta E_{O_2} = 1$ meV leads to an absorption coefficient change $\Delta\alpha = 100\,\text{cm}^{-1}$ after 30′, beyond which time the reduced mode amplitude relative to the QW μPL background precludes further quantitative estimates. As the initial linewidth is 0.8 meV, optical absorption by surface states becomes the dominant loss mechanism when oxygen is desorbed.

The changes in near-surface optical properties can be linked with past surface science studies of GaN surfaces with and without oxygen adsorption. In GaN, Fermi level pinning exists because of a high density ($\sim 1 \times 10^{14}\,\text{cm}^{-2}$)[31] of intrinsic, unoccupied surface states below the conduction band minimum [Fig. 2(d)].[32,33] Past experiments corroborate theoretical calculations; optically active surface states on $+c$- and m-plane GaN surfaces exist at 2.4 and 2.9 eV, respectively, less than the GaN bulk band gap of 3.4 eV.[31,34] Since the Fermi level must be flat in thermal equilibrium in the dark, a positive barrier (ϕ_b) is formed at the semiconductor-vacuum interface, as illustrated schematically in Fig. 2(d) for the m-plane.[33,34] A schematic with bent bands is also expected to remain applicable under 4.6 kW/cm^2 UV optical pumping because the photogenerated carrier concentration of $8 \times 10^{15}\,\text{cm}^{-3}$ remains below the donor concentration in the unintentionally doped GaN layers (*nid*, $N_d = 3 \times 10^{16}\,\text{cm}^{-3}$) due to fast nonradiative carrier recombination ($\tau_{PL} < 50$ ps) in the thin III-nitride on silicon epilayers at room temperature.

Oxygen desorption has been shown to modify intrinsic GaN surface states and, accordingly, the Fermi level pinning at the GaN surface. Past measurements confirm that ϕ_b can be changed following oxygen exposure on pristine GaN crystal facets: from 0.6–1.0 to 0.2 eV for the m-plane,[34,35] from 1.0 to 0.9 for the c-plane,[36] and from an unknown value to 1.1 eV for the a-plane.[37] Furthermore, the present experimental system likely exhibits additional extrinsic surface defects due to chemical contamination and damage from clean room processing, which could be removed or passivated by anisotropic wet etching[38,39] or atomic layer deposition[40] in future work. Although similar measurements do not exist for GaN, polarization dependent reflectance measurements of silicon[41] and GaAs surfaces[42] indicate that sub-gap optical absorption by surface states is strongest when the electric field vector is perpendicular to the surface. Therefore, one could expect the m-plane to be dominant for TE-like microdisk modes. In any case, the negatively charged surface is compensated by an adjacent, depleted space charge region (SCR), ensuring charge neutrality. Since oxygen

desorption modifies the Fermi level pinning, the SCR width changes in response; therefore, the doping dependence is studied in order to pinpoint the spatial region which causes the observed modes' redshift and broadening upon oxygen desorption.

B. Doping dependence

Doping the GaN epilayers changes the width w of the SCR created by Fermi level pinning at both the polar and nonpolar surfaces of n-GaN. w can be estimated in the abrupt junction approximation to be inversely proportional to the square root of the donor concentration (N_d)[7]

$$w = \sqrt{\frac{2\epsilon_0\epsilon_r}{q^2 N_d}\phi_b}, \quad (2)$$

where ϵ_0 is the vacuum permittivity, ϵ_r is the low frequency relative permittivity of the semiconductor, and q is the elementary charge. Therefore, the spectral changes induced by reversible oxygen desorption in nominally identical *nid* and heavily Si-doped (n^+, $N_d \approx 3\times10^{18}\,\text{cm}^{-3}$) GaN epilayers in the microdisks are compared. $w(t=0)$ is expected to be greater than 140 nm and 8 nm for *nid* and n^+ GaN, respectively. Taking the characteristic radial length scale of the whispering gallery resonances to be the inter-node distance of electromagnetic waves in the semiconductor, $L_{em} = \lambda/2n_{eff} \approx 100$ nm, substantial overlap between the SCR and the whispering gallery resonances is expected for *nid* GaN, while reduced overlap is expected for the n^+ material. Even in the unlikely scenario that ϕ_b were to increase from 0.2 eV to 1.0 eV, corresponding to full oxygen desorption for m-plane GaN, w would increase to 18 nm for n^+ doping, a value substantially smaller than L_{em}. Therefore, if the SCR were to comprise a dominant contribution to the optical changes during photodesorption, smaller redshift rates should be expected for the n^+ microdisks.

Figure 3 examines the doping dependence of oxygen desorption for *nid* (a) and n^+ (b) samples under 4.6 kW/cm^2 cw 325 nm optical pumping, vacuum $<1\times10^{-3}$ mbar, and at room temperature. Two additional samples were prepared side-by-side to minimize discrepancies originating from cleanroom processing. 4 μm diameter disks with 1.2 μm diameter silicon posts [Fig. 3(d)] were selected due to the smaller relative silicon post diameter on this batch of samples. The *nid* and n^+ doped microdisks' fastest shifting modes exhibit similar redshift rates of up to 1 meV over 10 min. Thus, the SCR does not appear to contribute substantially to the redshift, confirming that optical shifts induced by oxygen desorption are exclusively localized to a single region, the semiconductor surface.

The time dynamics differ for the *nid* and n^+ material: the *nid* microdisk resonances, as in Fig. 2, linearly redshift with time, whereas the n^+ redshift rates increase with time, exhibiting a linear time dependence only after about 10 min. This behavior can be attributed to poor hole transport because of the high dislocation density of thin III-nitride epilayers grown on silicon ($3\times10^{10}\,\text{cm}^{-2}$).[16] Outside the SCR, the minority carrier diffusion length is projected to be <20 nm.[43] Thus,

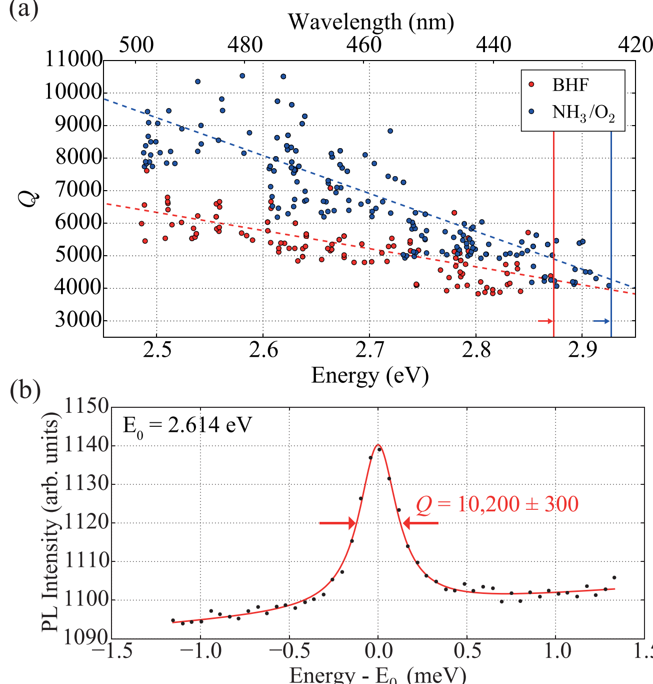

FIG. 4. Photoluminescence energy and surface treatment dependence of quality factor measured at 5 K under 325 nm cw optical pumping at 460 W/cm^2. Two surface treatments are examined sequentially on the same sample (a), 49% buffered hydrofluoric acid (red) followed by annealing in NH_3 and O_2 at 750 °C (blue). Dashed lines are linear regressions and solid lines show the energy cutoff. (b) μPL signal and Lorentzian fit for a high-Q mode at 2.6 eV. The spectrometer resolution corresponds to a Q of 14 000.

only holes photogenerated in or close to the depletion region near the semiconductor surface may contribute to the oxygen desorption phenomenon. Recent work suggests that transport from within the SCR to the surface is expected to occur on similar timescales to those presented here due to hopping via discrete states in the SCR.[44] Thus, the change in the redshift rate of the n^+ material with time may originate from an increase in the SCR width w beyond a threshold value corresponding to the characteristic transport length in the SCR. Most importantly, given that the presence of oxygen reduces surface state optical losses, the last experiment examines the effect of oxygen-based surface treatments.

C. Surface passivation

Following a literature review of cleaning techniques for c-plane GaN surfaces, two surface treatments are compared sequentially on the *nid* 3 μm diameter microdisks presented in Fig. 1(a). Preparation in 49% buffered hydrofluoric acid (BHF) for one minute and rapid thermal annealing in NH_3 and O_2 for 5 min each at 750 °C should be expected to yield surfaces with low and high oxygen content, respectively.[45–47] Figure 4 compares the energy dispersion of Q for the two surface treatments at 5 K and 460 W/cm^2 excitation intensity. Figure 4 reports the highest 15% of observed Q values over seven nominally identical microdisks in order to exclude higher order radial modes that may have substantial overlap with the absorptive silicon post. At 5 K, no photoinduced oxygen desorption is observed with the HeCd pump laser. Figure 4 reveals that the high oxygen content surface

treatment improves the maximum observed Q throughout the experimental spectral window to new state-of-the-art values for III-nitrides[24,48] exceeding 1×10^4 at 2.6 eV [Fig. 4(b)].

Interestingly, a high energy cutoff around 2.87 eV appears, which can be shifted to 2.92 eV by the surface treatment. Furthermore, the position of the high energy cutoff is consistent with past calculations and measurements pinpointing a peak joint density of surface states at 2.9–3.0 eV for m-plane GaN surfaces[33,34] and GaN nanowires.[49] Although one could argue that the losses are due to QW absorption which could be modified during thermal processing, the annealing temperature remains below the 880 °C threshold expected to alter InGaN/GaN QWs.[50] Therefore, this shift provides additional evidence that surface state absorption constitutes a major loss mechanism for GaN-based nanophotonic resonators at energies approaching 3.0 eV.

IV. CONCLUSION

To summarize, the importance of and control over optically active surface states in GaN microdisk optical resonators was demonstrated. At room temperature, nearly reversible oxygen desorption from the GaN surface under vacuum was induced by UV illumination. Oxygen desorption increased the optical losses and the refractive index in the blue spectral range. Doping-dependent oxygen desorption measurements support the conclusion that the spectral changes originated at the III-nitride surface. Oxygen-poor and oxygen-rich surface treatments were compared on the same microdisks, revealing that an oxygen-rich surface reduced optical losses. These findings bridge the gap between fundamental studies of GaN surfaces and practical devices, and may be of further importance for increasingly miniaturized nitride-based opto-electronics in research and industry, such as micro/nanowire LEDs and high power lasers,[51] for which GaN surface absorption may be highly detrimental.

SUPPLEMENTARY MATERIAL

See supplementary material for additional information on sample preparation and characterization. Additional sections detail micro-Raman and time-resolved photoluminescence experiments and calculations which support the arguments in the main text.

ACKNOWLEDGMENTS

This work was supported by the Swiss National Science Foundation through Grant No. 200020_162657. The authors would like to thank Martin Feneberg, Stefan Freytag, and Rüdiger Goldhahn from Otto von Guericke University in Magdeburg, Germany, for spectroscopic ellipsometry measurements and Momchil Minkov for help with the FDTD simulations. Discussions with Pierre Corfdir, Stefan Jagsch, and Bruno Gayral were helpful in identifying the oxygen desorption phenomenon.

[1]M. Mandl, X. Wang, T. Schimpke, C. Kölper, M. Binder, J. Ledig, A. Waag, X. Kong, A. Trampert, F. Bertram, J. Christen, F. Barbagini, E. Calleja, and M. Strassburg, Phys. Status Solidi RRL **7**, 800 (2013).
[2]S. Gradečak, F. Qian, Y. Li, H. G. Park, and C. M. Lieber, Appl. Phys. Lett. **87**, 173111 (2005).
[3]Y. Huang, X. Duan, Y. Cui, and C. M. Lieber, Nano Lett. **2**, 101 (2002).
[4]*GaN Transistors for Efficient Power Conversion*, edited by A. Lidow, J. Strydom, M. de Rooij, and D. Reusch (John Wiley & Sons Ltd, Chichester, United Kingdom, 2014), pp. 1–18.
[5]C. Xiong, W. Pernice, C. Schuck, and H. X. Tang, Int. J. High Speed Electron. Syst. **23**, 1450001 (2014).
[6]L. J. Brillson, *Surfaces and Interfaces of Electronic Materials*, 1st ed. (Wiley-VCH, Weinheim, DE, 2012), pp. 37–62.
[7]S. Sze and K. Ng, *Semiconductor Devices: Physics and Technology*, 3rd ed. (Wiley Interscience, Hoboken, NJ, 2007), pp. 134–196.
[8]E. Yablonovitch, C. J. Sandroff, R. Bhat, and T. Gmitter, Appl. Phys. Lett. **51**, 439 (1987).
[9]M. Borselli, T. J. Johnson, and O. Painter, Appl. Phys. Lett. **88**, 131114 (2006).
[10]B. Guha, F. Marsault, F. Cadiz, L. Morgenroth, V. Ulin, V. Berkovitz, A. Lemaître, C. Gomez, A. Amo, S. Combrié, B. Gérard, G. Leo, and I. Favero, Optica **4**, 218 (2017).
[11]S. L. McCall, A. F. J. Levi, R. E. Slusher, S. J. Pearton, and R. A. Logan, Appl. Phys. Lett. **60**, 289 (1992).
[12]E. Yablonovitch, Phys. Rev. Lett. **58**, 2059 (1987).
[13]S. John, Phys. Rev. Lett. **58**, 2486 (1987).
[14]F. Vollmer and S. Arnold, Nat. Methods **5**, 591 (2008).
[15]N. Vico Triviño, R. Butté, J.-F. Carlin, and N. Grandjean, Nano Lett. **15**, 1259 (2015).
[16]I. Rousseau, I. Sánchez-Arribas, K. Shojiki, J.-F. Carlin, R. Butté, and N. Grandjean, Phys. Rev. B **95**, 125313 (2017).
[17]M. Minkov and V. Savona, Sci. Rep. **4**, 5124 (2014).
[18]S. Sergent, M. Arita, S. Kako, S. Iwamoto, and Y. Arakawa, Appl. Phys. Lett. **100**, 121103 (2012).
[19]D. Néel, I. Roland, X. Checoury, M. El Kurdi, S. Sauvage, C. Brimont, T. Guillet, B. Gayral, F. Semond, and P. Boucaud, Adv. Nat. Sci.: Nanosci. Nanotechnol. **5**, 023001 (2014).
[20]J. Sellés, C. Brimont, G. Cassabois, P. Valvin, T. Guillet, I. Roland, Y. Zeng, X. Checoury, P. Boucaud, M. Mexis, F. Semond, and B. Gayral, Sci. Rep. **6**, 21650 (2016).
[21]T. J. Puchtler, A. Woolf, T. Zhu, D. Gachet, E. L. Hu, and R. A. Oliver, ACS Photonics **2**, 137 (2015).
[22]D. Simeonov, E. Feltin, A. Altoukhov, A. Castiglia, J.-F. Carlin, R. Butté, and N. Grandjean, Appl. Phys. Lett. **92**, 171102 (2008).
[23]A. C. Tamboli, E. D. Haberer, R. Sharma, K. H. Lee, S. Nakamura, and E. L. Hu, Nat. Photonics **1**, 61 (2007).
[24]A. Woolf, T. Puchtler, I. Aharonovich, T. Zhu, N. Niu, D. Wang, R. Oliver, and E. L. Hu, Proc. Natl. Acad. Sci. U.S.A. **111**, 14042 (2014).
[25]F. Tabataba-Vakili, I. Roland, T.-M. Tran, X. Checoury, M. El Kurdi, S. Sauvage, C. Brimont, T. Guillet, S. Rennesson, J.-Y. Duboz, F. Semond, B. Gayral, and P. Boucaud, Appl. Phys. Lett. **111**, 131103 (2017).
[26]*FDTD Solutions v. 8.12.501* (Lumerical Solutions, Inc., Vancouver, BC, Canada, 2015), available at http://www.lumerical.com/tcad-products/fdtd/.
[27]D. F. Edwards, in *Handbook of Optical Constants of Solids*, edited by E. Palik (Academic Press, Orlando, FL, USA, 1985), pp. 547–569.
[28]M. Foussekis, A. A. Baski, and M. A. Reshchikov, Appl. Phys. Lett. **94**, 162116 (2009).
[29]C. Pfüller, O. Brandt, F. Grosse, T. Flissikowski, C. Chèze, V. Consonni, L. Geelhaar, H. T. Grahn, and H. Riechert, Phys. Rev. B **82**, 045320 (2010).
[30]R. E. Slusher, A. F. J. Levi, U. Mohideen, S. L. McCall, S. J. Pearton, and R. A. Logan, Appl. Phys. Lett. **63**, 1310 (1993).
[31]M. A. Reshchikov, M. Foussekis, and A. A. Baski, J. Appl. Phys. **107**, 113535 (2010).
[32]C. G. Van de Walle and D. Segev, J. Appl. Phys. **101**, 081704 (2007).
[33]M. Landmann, E. Rauls, W. Schmidt, M. Neumann, E. Speiser, and N. Esser, Phys. Rev. B **91**, 035302 (2015).
[34]M. Himmerlich, A. Eisenhardt, S. Shokhovets, S. Krischok, J. Räthel, E. Speiser, M. D. Neumann, A. Navarro-Quezada, and N. Esser, Appl. Phys. Lett. **104**, 171602 (2014).
[35]V. Portz, M. Schnedler, H. Eisele, R. E. Dunin-Borkowski, and P. Ebert, “Electron affinity and surface states of GaN m-plane facets: Implication for electronic self-passivation,” Phys. Rev. B (to be published).
[36]J. Long and V. Bermudez, Phys. Rev. B **66**, 121308 (2002).
[37]S. Chevtchenko, X. Ni, Q. Fan, A. A. Baski, and H. Morkoç, Appl. Phys. Lett. **88**, 122104 (2006).

[38]W. Chen, X. Wen, M. Latzel, M. Heilmann, J. Yang, X. Dai, S. Huang, S. Shrestha, R. Patterson, S. Christiansen, and G. Conibeer, ACS Appl. Mater. Interfaces **8**, 31887 (2016).
[39]H. Sun, M. K. Shakfa, M. Muhammed, B. Janjua, K.-H. Li, R. Lin, T. K. Ng, I. S. Roqan, B. S. Ooi, and X. Li, "Surface-passivated AlGaN nanowires for enhanced luminescence of ultraviolet light emitting diodes," ACS Photonics (published online).
[40]P. Neuderth, P. Hille, J. Schörmann, A. Frank, C. Reitz, S. Martí-Sánchez, M. de la Mata, M. Coll, J. Arbiol, R. Marschall, and M. Eickhoff, J. Mater. Chem. A **6**, 565 (2018).
[41]M. A. Olmstead and N. M. Amer, Phys. Rev. Lett. **52**, 1148 (1984).
[42]V. Berkovits, I. Makarenko, T. Minashvili, and V. Safarov, Solid State Commun. **56**, 449 (1985).
[43]K. Kumakura, T. Makimoto, N. Kobayashi, T. Hashizume, T. Fukui, and H. Hasegawa, Appl. Phys. Lett. **86**, 052105 (2005).
[44]A. Winnerl, R. N. Pereira, and M. Stutzmann, J. Appl. Phys. **121**, 205307 (2017).
[45]V. Bermudez, J. Appl. Phys. **80**, 1190 (1996).
[46]V. Bermudez, Appl. Surf. Sci. **119**, 147 (1997).
[47]S. King, J. Barnak, M. Bremser, K. Tracy, C. Ronning, R. Davis, and R. Nemanich, J. Appl. Phys. **84**, 5248 (1998).
[48]M. Mexis, S. Sergent, T. Guillet, C. Brimont, T. Bretagnon, B. Gil, F. Semond, M. Leroux, D. Néel, S. David, X. Chécoury, and P. Boucaud, Opt. Lett. **36**, 2203 (2011).
[49]R. Calarco, M. Marso, T. Richter, A. I. Aykanat, R. Meijers, A. v. d. Hart, T. Stoica, and H. Lüth, Nano Lett. **5**, 981 (2005).
[50]N. A. K. Kaufmann, A. Dussaigne, D. Martin, P. Valvin, T. Guillet, B. Gil, F. Ivaldi, S. Kret, and N. Grandjean, Semicond. Sci. Technol. **27**, 105023 (2012).
[51]C. C. Kim, Y. Choi, Y. H. Jang, M. K. Kang, M. Joo, and M. S. Noh, Proc. SPIE **6894**, 68940O (2008).